

Fault Simulation for Superconducting Quantum Circuits

Mingyu Huang

*State Key Laboratory of Computer Science
Institute of Software, Chinese Academy of Sciences
Beijing, China
huangmy@ios.ac.cn*

Wang Fang

*State Key Laboratory of Computer Science
Institute of Software, Chinese Academy of Sciences
Beijing, China
fangw@ios.ac.cn*

Ji Guan

*State Key Laboratory of Computer Science
Institute of Software, Chinese Academy of Sciences
Beijing, China
guanji1992@gmail.com*

Mingsheng Ying

*State Key Laboratory of Computer Science
Institute of Software, Chinese Academy of Sciences
Department of Computer Science and Technology, Tsinghua University
Beijing, China
yingms@ios.ac.cn*

Abstract—This paper introduces a fast fault simulation algorithm for superconducting quantum circuits with realistic fault models based on real defect behavior or control errors of the circuits. The algorithm is developed on a novel tensor network representation of the fault models with fast tensor network computation. The effectiveness and utility of the algorithm are demonstrated by experimenting on a series of practical quantum circuits executed on Google’s *Sycamore* quantum superconducting processor. As a result, up to 225 qubits (for the variational quantum circuits) are handled (within about 15 minutes), outperforming state-of-the-art fault simulation algorithms in both efficiency and scalability.

Index Terms—Quantum computing, quantum circuits, fault simulation, tensor network

I. INTRODUCTION

Nowadays, various quantum processors have been manufactured, and quantum supremacy has been achieved. Among the existing hardware implementations of quantum processors, superconducting quantum computing is one of the most promising routines. Specifically, superconducting quantum bits (qubits) have faster gate time, which means the execution of the quantum circuit will be faster. Additionally, superconducting implementation is also capable of using a large number of qubits. The superconducting processor *Sycamore* of Google with 53 qubits is the first processor that achieves quantum supremacy (beyond classical computing) [1]. After that, University of Science and Technology of China implemented a 2-dimensional quantum random walk on a 62-qubit superconducting quantum processor [2]. Thus, the superconducting quantum computing implementation may bring practical applications to the current NISQ (Noisy Intermediate-Scale Quantum) era [3], where quantum processors contain 50 to a few hundred noisy qubits.

The core of the processors is the circuits for executing computational tasks. Before the circuits are physically built, simulation is essential in digital circuit verification, test development, design debugging, and diagnosis. In particular, *fault simulation* is to simulate faulty digital circuits with two main objectives: one is fault-free (logic) simulation to help the designer verify that the design of digital circuits conforms to the intended functional specifications; the other is to determine the efficiency of test patterns in detecting the modeled faults of interest, with such patterns being usually generated by automatic test pattern generators (ATPG) [4], [5]. Now fault simulation can be efficiently applied to large-scale integrated circuits and has become a standard technique integrated into electronic design automation (EDA).

Currently, in quantum computing, however, physicists usually experimentally build the designed quantum circuits and then estimate their performance in the presence of *quantum faults*. Here, the quantum faults come from the inaccuracy of the control pulse and the surrounding environment, which is inevitable in the NISQ era. For example, a circuit with four qubits and four controlled quantum logic gates was implemented in [6] for an experiment of HHL algorithm [7], which could exponentially speed up solving linear systems over classical computers. The performance test for three different input states shows that compared to the ideal outcomes, the output states have fidelities of 99.3%, 82.5%, and 83.6%, respectively. Google’s *Sycamore* has used a similar way to confirm quantum supremacy on sampling a quantum circuit with cross-entropy benchmark fidelity 0.2% [1].

Fault simulation of quantum circuits (on classical computers) before physically building them is helpful and more affordable due to the expensive resource and strict conditions (e.g., the environmental temperature must be close to absolute zero) of experimentally implementing quantum circuits and the uncertainty of reading out outputs on real quantum devices. Therefore, developing fault simulation algorithms for (superconducting) quantum circuits is urgent and necessary. However, a direct generalization of the existing fault simulation method for classical circuits to quantum circuits is expected to be unsuccessful. One primary reason is that quantum fault simulation is generally quantitative rather than qualitative as classical fault simulation: the inputs/outputs of quantum circuits are vectors or matrices of complex numbers, while those of classical circuits are boolean values — 0 or 1. This fundamental difference requires quantum fault simulation to be built in its own way.

Quantum Fault Simulation Algorithms: We first recall the state-of-the-art simulation algorithms for noiseless and noisy quantum circuits. For both cases, a direct method is to calculate the transitions of the state vector or density matrix representation through a sequence of quantum gates modeled by unitary matrices. This method is simple and usually integrated into software development kits for quantum computing (e.g., Qiskit, Cirq, etc.). However, the exponential number of terms in these representations limits the number of qubits that can be simulated. For overcoming this issue, one of the most popular methods is to use a data structure, called *tensor network*, to catch the locality (a quantum gate is only applied on 1 or 2 qubits) and regularity (the pattern of quantum gates in practical circuits is regular) of quantum circuits and has been successively used in the

simulation of sizeable noiseless quantum circuits [8]–[13]. However, the tensor network method cannot directly simulate noisy quantum circuits. Another approach is the Decision Diagram-based (DD-base) method [14], [15], which is generally more lightweight than the tensor network-based one. It stores all amplitudes of a state in a compact data structure, using less memory and performing better on circuits with simpler structures. However, most of these methods work well for the circuits which can keep the size of the data structures small for each intermediate state in the simulating process. They can achieve satisfactory performance in full amplitude simulation of this kind of circuit. However, superconducting quantum circuits compose of gates with arbitrary parameters, and the performance of such methods on these circuits is ineffective [14], [16]. Although the DD-based methods can be adapted to support noisy quantum circuit simulation [17], the extra noise operator leads to a high cost of runtime.

Current superconducting quantum processors have a relatively large number of qubits, and most circuits include gates with arbitrary rotation angles, this motivates us to develop a new simulation algorithm based on the tensor network representation of noisy quantum circuits to perform fault simulation on the superconducting quantum circuits.

Contributions of This Paper: The tensor network-based techniques cannot be immediately used to simulate faulty quantum circuits as quantum faults affected by quantum noises cannot be directly represented by tensor networks. We solve this problem by representing a faulty quantum circuit in a *double-size* tensor network. An algorithm is developed and implemented with Google TensorNetwork [18] to simulate all kinds of quantum faults. Our experimental results show that with our new method, the simulated size of practical faulty superconducting quantum circuits can be boosted up to 225 qubits for that of the QAOA algorithm.

II. FAULT MODELS

As a basis of our work, this section aims to present fault models of superconducting quantum circuits [19].

We start by recalling some basic concepts of quantum circuits. Ideally, a quantum computer without noise is a closed system. In this case, quantum data are mathematically modeled as complex unit vectors in a 2^n -dimensional Hilbert (linear) space \mathcal{H} . Such a quantum datum is usually called a *pure state* and written as $|\psi\rangle$ in the Dirac notation, and n represents the number of involved *quantum bits (qubits)*. Specifically, a qubit is a quantum datum in a 2-dimensional Hilbert space, denoted by $|q\rangle = \begin{pmatrix} a \\ b \end{pmatrix} = a|0\rangle + b|1\rangle$

with $|0\rangle = \begin{pmatrix} 1 \\ 0 \end{pmatrix}$ and $|1\rangle = \begin{pmatrix} 0 \\ 1 \end{pmatrix}$, where complex numbers a and b satisfy the normalization condition $|a|^2 + |b|^2 = 1$. Here, the orthonormal basis $\{|0\rangle, |1\rangle\}$ of the Hilbert space corresponds to the values $\{0, 1\}$ of a bit in classical computers. A quantum computing task is implemented by a *quantum circuit*, which is mathematically represented by a $2^n \times 2^n$ unitary matrix U , i.e., $U^\dagger U = UU^\dagger = I_n$, where U^\dagger is the (entry-wise) conjugate transpose of U and I_n is the identity matrix on \mathcal{H} . For an input n -qubit datum $|\psi\rangle$, the output of the circuit is a datum of the same size: $|\psi'\rangle = U|\psi\rangle$.

Like its classical counterpart, a quantum circuit U consists of a sequence (product) of *quantum logic gates* U_i , i.e., $U = U_d \cdots U_1$. Here d is the depth of the circuit U . Each gate U_i only non-trivially operates on one or two qubits. We list commonly used 1-qubit gates in Table I. Arbitrary 1-qubit gates can be decomposed into 1-qubit rotation gates $R_x(\theta)$, $R_y(\theta)$ and $R_z(\theta)$ with rotation parameter θ ,

TABLE I: 1-QUBIT GATE

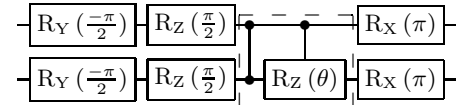
H	$\frac{1}{\sqrt{2}} \begin{pmatrix} 1 & 1 \\ 1 & -1 \end{pmatrix}$	X (σ_x)	$\begin{pmatrix} 0 & 1 \\ 1 & 0 \end{pmatrix}$
Y (σ_y)	$\begin{pmatrix} 0 & -i \\ i & 0 \end{pmatrix}$	Z (σ_z)	$\begin{pmatrix} 1 & 0 \\ 0 & -1 \end{pmatrix}$
T	$\begin{pmatrix} 1 & 0 \\ 0 & e^{i\pi/4} \end{pmatrix}$	$R_x(\theta)$	$\begin{pmatrix} \cos \frac{\theta}{2} & -i \sin \frac{\theta}{2} \\ -i \sin \frac{\theta}{2} & \cos \frac{\theta}{2} \end{pmatrix}$
$R_y(\theta)$	$\begin{pmatrix} \cos \frac{\theta}{2} & -\sin \frac{\theta}{2} \\ \sin \frac{\theta}{2} & \cos \frac{\theta}{2} \end{pmatrix}$	$R_z(\theta)$	$\begin{pmatrix} e^{-i\theta/2} & 0 \\ 0 & e^{i\theta/2} \end{pmatrix}$

and superconducting quantum processors implement arbitrary 1-qubit gate by executing a sequence of these rotation gates. In addition, for any 1-qubit logic gate U , we can generate a 2-qubit logic gate — controlled- U (CU) gate, applying U on the second (target) qubit if and only if the first (control) qubit is $|1\rangle$. Specifically, the controlled-Z (CZ) gate is commonly used in superconducting quantum circuits.

$$\text{CU} = \begin{array}{c} \text{---} \\ | \\ \text{---} \end{array} \begin{array}{c} | \\ \text{---} \\ \boxed{U} \\ \text{---} \\ | \\ \text{---} \end{array} \quad \text{CZ} = \begin{array}{c} \text{---} \\ | \\ \text{---} \end{array} \begin{array}{c} | \\ \text{---} \\ | \\ \text{---} \end{array} = \begin{pmatrix} 1 & 0 & 0 & 0 \\ 0 & 1 & 0 & 0 \\ 0 & 0 & 1 & 0 \\ 0 & 0 & 0 & -1 \end{pmatrix}$$

Now, we are ready to introduce fault models for superconducting quantum circuits. By the principle of quantum mechanics, faults in quantum circuits fall into two classes — unitary faults and super-operator faults.

Unitary Faults: Elementary 2-qubit gates (e.g. CZ gate), are implemented by adding control pulses to effective Hamiltonians in real superconducting quantum chips. A typical CZ gate could be realized by modulating the frequency of the control qubit, which is called a σ_z control. Additional dynamical phases are accumulated in the pulse duration. However, the σ_z control requires fine-tuning. Therefore, errors in the pulse parameters will lead to undesired $R_z(\theta)$, accounting for the fidelity loss. The effect of this fault is appending a controlled- R_z gate after the ideal CZ gate, as shown in the dashed box of the following circuit for a quantum approximate optimization algorithm (QAOA) [20], which is a variational quantum algorithm for solving combinatorial optimization problems. Such a fault is called a *unitary fault*, which is represented by a unitary matrix.



A 2-qubit QAOA circuit with a unitary fault on CZ gate

Super-operator Faults: In the current NISQ era, quantum noise is unavoidable, we have to consider the noisy effect on quantum circuits. In this case, uncertainty will be brought in quantum computing such that quantum states became mixed instead of pure states. A *mixed state* is considered as an ensemble $\{(p_k, |\psi_k\rangle)\}$, meaning the quantum system is in state $|\psi_k\rangle$ with probability p_k . Mathematically, it can be described by a $2^n \times 2^n$ density matrix ρ (Hermitian positive semidefinite matrix with unit trace¹) on \mathcal{H} : $\rho = \sum_k p_k |\psi_k\rangle\langle\psi_k|$, where $\langle\psi_k|$ is the conjugate transpose of $|\psi_k\rangle$, i.e., $\langle\psi_k| = |\psi_k\rangle^\dagger$. For convenience, we use ψ to denote the density operator of pure state $|\psi\rangle\langle\psi|$. We write $\mathcal{D}(\mathcal{H})$ for the set of all (mixed) quantum states on \mathcal{H} . In this situation, a computational task starting at a mixed state ρ is finished by a mapping \mathcal{E} : $\rho' = \mathcal{E}(\rho)$, where \mathcal{E} is the noisy implementation of the noiseless quantum circuit U . Such a \mathcal{E} is called

¹ ρ has unit trace if $\text{tr}(\rho) = 1$, where trace $\text{tr}(\rho)$ of ρ is defined as the summation of diagonal elements of ρ .

a *super-operator*, and admits a *Kraus matrix form* [21]: there exists a finite set $\{E_k\}_{k \in \mathcal{K}}$ of matrices on \mathcal{H} such that

$$\mathcal{E}(\rho) = \sum_{k \in \mathcal{K}} E_k \rho E_k^\dagger \quad \text{with} \quad \sum_{k \in \mathcal{K}} E_k^\dagger E_k = I_n,$$

where $\{E_k\}_{k \in \mathcal{K}}$ is called *Kraus matrices* of \mathcal{E} . Briefly, \mathcal{E} is represented as $\mathcal{E} = \{E_k\}_{k \in \mathcal{K}}$. Similar to noiseless quantum circuit U , noisy quantum circuit \mathcal{E} also consists of a sequence (mapping composition) of (noisy) gates $\{\mathcal{E}_i\}$, i.e., $\mathcal{E} = \mathcal{E}_d \circ \dots \circ \mathcal{E}_1$, where each \mathcal{E}_i is either a noiseless gate or a noisy one. The noisy one is called a *super-operator fault*, which is represented by Kraus matrices.

In superconducting quantum hardware, decoherence is a typical noisy fault resulting from the surrounding environment of the hardware. Decoherence can be mathematically explained as the decay effect of the off-diagonal element in the density matrices of mixed states. The decay comes from amplitude damping and phase damping.

(1) Amplitude damping \mathcal{E}_a is a super-operator fault describing the effect that the energy of excited states gradually decreases, which has Kraus matrices:

$$E_{a,1} = \begin{pmatrix} 1 & 0 \\ 0 & e^{-\Delta t/2T_1} \end{pmatrix}, \quad E_{a,2} = \begin{pmatrix} 0 & \sqrt{1 - e^{-\Delta t/T_1}} \\ 0 & 0 \end{pmatrix}$$

where T_1 is the energy relaxation time and Δt is the gate time [19].

(2) Phase damping \mathcal{E}_p is also a super-operator fault refers to pure dephasing, which is the off-diagonal elements decay without affecting the population of diagonal elements. Phase damping can be described by three Kraus matrices:

$$E_{p,0} = e^{-\Delta t/2T_\varphi} I,$$

$$E_{p,1} = \sqrt{1 - e^{-\Delta t/T_\varphi}} |0\rangle\langle 0|, \quad E_{p,2} = \sqrt{1 - e^{-\Delta t/T_\varphi}} |1\rangle\langle 1|$$

where T_φ is defined by $\frac{1}{T_\varphi} = \frac{1}{T_2} - \frac{1}{2T_1}$ and T_2 is total dephasing time [19]. Decoherence \mathcal{E}_D is the composition of these two super-operators, i.e. $\mathcal{E}_D = \mathcal{E}_p \circ \mathcal{E}_a$.

At the end of quantum circuits, we cannot directly observe a qubit as it is physically a particle at the microscopic scale (near or less than 10^{-9} meters). The only way allowed by quantum mechanics to extract classical information is through a quantum measurement, which is mathematically modeled by a set $\{P_i\}_{i \in \mathcal{O}}$ of projection matrices on its state (Hilbert) space \mathcal{H} with \mathcal{O} being the set of outputs and $\sum_{i \in \mathcal{O}} P_i = I_n$. This observing process is probabilistic: for a given quantum state ρ , a measurement outcome $i \in \mathcal{O}$ is obtained with probability $p_i = \text{tr}(P_i \rho)$.

III. FAULT SIMULATION OF QUANTUM CIRCUITS

As illustrated in Fig. 1, the result of fault simulation works for fault detection and diagnosis. In this section, we first introduce fault detection and diagnosis for quantum circuits, then formulate the simulation problem in our work.

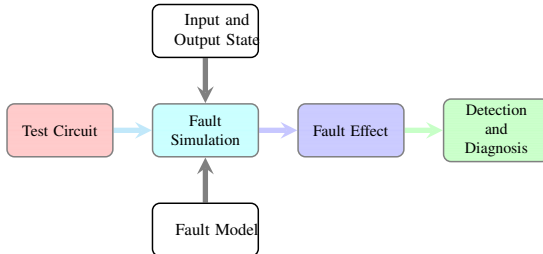


Fig. 1: Workflow of Fault Detection.

Fault Detection and Diagnosis for Quantum Circuits: Following the strategy of fault detection for classical digital circuits, for each

modeled fault of an ideal quantum circuit U , a carefully designed test state $|\psi_t\rangle$ is applied to a faulty circuit \mathcal{E}_f and then the output state $\mathcal{E}(\psi_t)$ is observed by a measurement $\{P_i\}_{i \in \mathcal{O}}$ according to each $|\psi_t\rangle$ to get the probability distribution $\{\text{tr}(P_i \mathcal{E}_f(\psi_t))\}_{i \in \mathcal{O}}$ of outcomes \mathcal{O} . If the distribution matches the expected one $\{\text{tr}(P_i U(\psi_t))\}_{i \in \mathcal{O}}$ for $U = \{U\}$, then such fault is deemed not to be present in U . Furthermore, if all tests corresponding to different modeled faults pass, the circuit U is guaranteed to contain no modeled faults. On the other hand, such test information (the probability distributions of measurement outcomes) can be used to find which modeled fault appears or which gate is faulty. This problem is known as the diagnosis of faulty quantum circuits (for more details, see [22]–[24], including how to generate such test states $|\psi_t\rangle$ and measurement $\{P_i\}_{i \in \mathcal{O}}$). It is formally defined as follows.

Definition 1: Given a faulty quantum circuit \mathcal{E}_f , a test state $|\psi_t\rangle$ and a measurement $\{P_i\}_{i \in \mathcal{O}}$, the fault simulation for detection and diagnosis is to compute probabilities $\text{tr}(P_i \mathcal{E}_f(\psi_t))$ for all $i \in \mathcal{O}$.

Note that P_i is the projection onto some subspace \mathcal{H}_i of \mathcal{H} : $P_i |\psi\rangle = |\psi\rangle$ for all $|\psi\rangle \in \mathcal{H}_i$; $P_i |\psi\rangle = 0$ for all $|\psi\rangle \in \mathcal{H}_i^\perp$, the orthogonal complement of \mathcal{H}_i . Thus, if $\{|\phi_{ik}\rangle\}$ is an orthonormal basis of \mathcal{H}_i , then P_i admits the *eigenvalue decomposition*: $P_i = \sum_k |\phi_{ik}\rangle\langle\phi_{ik}|$. With this decomposition, we have:

$$\begin{aligned} \text{tr}(P_i \mathcal{E}_f(\psi_t)) &= \text{tr}\left(\sum_k |\phi_{ik}\rangle\langle\phi_{ik}| \mathcal{E}_f(\psi_t)\right) \\ &= \sum_k \langle\phi_{ik}|\mathcal{E}_f(\psi_t)|\phi_{ik}\rangle \end{aligned}$$

Fault Effect of Quantum Circuits: In the field of fault detection and diagnosis, the projection P_i is usually defined by a pure state $|\phi_i\rangle$, i.e., $P_i = |\phi_i\rangle\langle\phi_i|$ [23], [24]. Subsequently, what we need to calculate is just $\langle\phi_i|\mathcal{E}_f(\psi_t)|\phi_i\rangle$ for all $i \in \mathcal{O}$. Back to the general case of calculating $\text{tr}(P_i \mathcal{E}_f(\psi_t))$ for all $i \in \mathcal{O}$, we only need to compute $\langle\phi_{ik}|\mathcal{E}_f(\psi_t)|\phi_{ik}\rangle$ in parallel for each i and k . As a result, we summarize the task of our fault simulation as *fault effect* in the following.

Definition 2: Given a faulty quantum circuit \mathcal{E}_f , a test state $|\psi_t\rangle$ and an measurement defined by state $|\psi_e\rangle$, the simulation for fault effect of \mathcal{E}_f on $|\psi_t\rangle$ is to compute $\langle\psi_e|\mathcal{E}_f(\psi_t)|\psi_e\rangle$.

Recall that the fidelity between two quantum states ρ and σ is:

$$F(\rho, \sigma) = [\text{tr}(\sqrt{\rho^{1/2} \sigma \rho^{1/2}})]^2.$$

In particular, for pure state $\psi = |\psi\rangle\langle\psi|$ and mixed state σ , $F(\psi, \sigma) = \langle\psi|\sigma|\psi\rangle$. As a result, the fault effect we defined is $\langle\psi_e|\mathcal{E}_f(\psi_t)|\psi_e\rangle = F(\psi_e, \mathcal{E}_f(\psi_t))$. Since the fidelity measures how close two quantum states (density operators) are, observe that if we choose $|\psi_e\rangle$ as the expected output state $U|\psi_t\rangle$, the fault effect just measures how close the real output state is with the expected output state. Thus instead of providing essential information for fault detection, fault simulation can also be used to predict the performance of quantum circuits under noise, such as that for the HHL algorithm mentioned in the introduction section.

IV. FAST FAULT SIMULATION ALGORITHM

In this section, we present our tensor network-based fast fault simulation algorithm for computing fault effect $F(\psi_e, \mathcal{E}_f(\psi_t))$.

Tensor Network Contraction: For a better understanding, let us explain tensor network contraction by tensor diagram notation in the context of quantum circuits (see [25] for more details). Briefly, a tensor is a multi-dimensional array of complex numbers and is a labeled box with zero or more open output legs. Each leg labeled by an index (e.g., i, j, k) represents a dimension of the

array, and a complex number is a tensor without legs. For example, the following notations represent a complex number (e.g., $e^{i\pi/4}$), a vector (e.g., pure state $|\psi\rangle$), a matrix (e.g., quantum gate U) and a set of matrices (e.g. quantum noise $\mathcal{E} = \{E_k\}_{k \in \mathcal{K}}$), respectively.

$$\begin{array}{c} e^{i\pi/4} \\ \boxed{e^{i\pi/4}} \end{array} \quad j - \boxed{|\psi\rangle} \quad i - \boxed{U} - j \quad i - \boxed{\mathcal{E}} - j$$

Furthermore, if multiple tensors exist in a diagram, then we call them a tensor network. In this case, we can contract them by linking their legs with the same indexes. This operation is known as *tensor network contraction*, which is a generalization of matrix (and vector) multiplication. For example, vector-matrix-vector product $\langle\phi|U|\psi\rangle = \sum_{ij} a_i U_{ij} b_j$ for $|\phi\rangle = (a_1, \dots, a_{2^n})^\dagger$ and $|\psi\rangle = (b_1, \dots, b_{2^n})^\top$, and matrix-matrix product $(AB)_{ik} = \sum_j A_{ij} B_{jk}$ are illustrated as the following two tensor contractions:

$$\begin{array}{ll} \langle\phi| \xrightarrow{i} \boxed{U} \xrightarrow{j} |\psi\rangle & = \quad \langle\phi|U|\psi\rangle \\ i - \boxed{A} \xrightarrow{j} \boxed{B} - k & = \quad i - \boxed{AB} - k \end{array}$$

The above two diagrams on the left are instances of tensor networks. Indeed, all quantum circuits in the previous sections can be easily represented as tensor networks, where a gate is a tensor and each leg of the gate is labeled by an index in $\{0, 1\}$.

The benefit of representing quantum circuits by tensor networks is that tensor networks can exploit the regularity and locality contained in the structure of quantum circuits (but matrix representation cannot). Complexity of tensor network contraction for a q -local-interacting quantum circuit is $T^{O(1)} \exp[O(qd)]$ [26], where T is the number of gates (tensors), d is the depth in the circuit (tensor network), and a circuit is q -local-interacting if under a linear ordering of its qubits, each gate acts only on qubits within distance q . Even though the worse case (presented in the complexity) is exponential in d , there are a bulk of efficient algorithms to implement tensor network contraction for practical large-size quantum circuits (e.g. [8]–[12]).

Now we are ready to present our quantum fault simulation algorithm. The key idea is to convert the noisy quantum circuits into a double-size tensor network (Algorithm 1).

Fast Fault Simulation Algorithm: We can compute fault effect $F(\psi_e, \mathcal{E}_f(\psi_t))$ in the following way.

$$\begin{aligned} F(\psi_e, \mathcal{E}_f(\psi_t)) &= \langle\psi_e| \mathcal{E}_f(\psi_t) |\psi_e\rangle = \text{tr}(\psi_e \mathcal{E}_f(\psi_t)) \\ &= \langle\Omega| [\langle\psi_e^*| \langle\psi_e^*| \otimes \mathcal{E}_f(\psi_t)] |\Omega\rangle \\ &= \langle\Omega| [\langle\psi_e^*| \langle\psi_e| \otimes \mathcal{E}_d \circ \dots \circ \mathcal{E}_1(\psi_t)] |\Omega\rangle \\ &= \langle\psi_e^*| \otimes \langle\psi_e| (M_{\mathcal{E}_d} \dots M_{\mathcal{E}_1}) |\psi_e^*\rangle \otimes |\psi_t\rangle \end{aligned}$$

where $|\psi_e^*\rangle$ is the entry-wise conjugate of $|\psi_e\rangle$, $|\Omega\rangle$ is the (unnormalized) maximal entangled state, i.e., $|\Omega\rangle = \sum_j |j\rangle \otimes |j\rangle$ with $\{|j\rangle\}$ being an orthonormal basis of Hilbert space \mathcal{H} , and $M_{\mathcal{E}} = \sum_k E_k \otimes E_k^*$ for $\mathcal{E} = \{E_k\}$ is called the *matrix representation* of \mathcal{E} [27].

Algorithm 1 FastFaultSimulation($\mathcal{E}_f, |\psi_t\rangle, |\psi_e\rangle$)

Input: A faulty quantum circuit $\mathcal{E}_f = \mathcal{E}_d \circ \dots \circ \mathcal{E}_1$ with $\mathcal{E}_i = \{E_{ik}\}_{k \in \mathcal{K}_i}$ for $d \geq i \geq 1$, a test state $|\psi_t\rangle$ and an expected output $|\psi_e\rangle$.

Output: The fault effect $F(\psi_e, \mathcal{E}_f(\psi_t))$

1: Computing $X = \langle\psi_e^*| \otimes \langle\psi_e| (M_{\mathcal{E}_d} \dots M_{\mathcal{E}_1}) |\psi_e^*\rangle \otimes |\psi_t\rangle$ by calling a tool for tensor network contraction

2: **return** X

We observe that $M_{\mathcal{E}} = \sum_{k \in \mathcal{K}} E_k \otimes E_k^*$ can be represented by the following left tensor network. In particular, for a unitary $\mathcal{U} = \{U\}$,

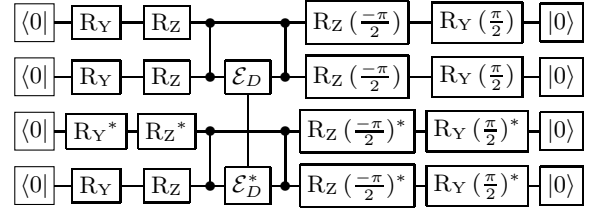


Fig. 2: Circuit for calculating fidelity of the 2-qubit QAOA circuit in Section II with decoherence noise \mathcal{E}_D by appending $|\psi_e\rangle = U|\psi_t\rangle$ to the end of circuit and redundant gates are canceled out.

$M_{\mathcal{E}}$ is depicted as the right tensor network.

$$M_{\mathcal{E}} = \sum_{k \in \mathcal{K}} E_k \otimes E_k^* = \boxed{\mathcal{E}} \quad M_{\mathcal{U}} = U \otimes U^* = \boxed{U} - \boxed{U^*}$$

With this observation, we get a serial connection of the two tensor networks representing n -qubit circuits \mathcal{E}_f and \mathcal{E}_f^* . Subsequently, we can compute $\langle\psi_e^*| \otimes \langle\psi_e| (M_{\mathcal{E}_d} \dots M_{\mathcal{E}_1}) |\psi_e^*\rangle \otimes |\psi_t\rangle$ by contracting a tensor network with double size ($2n$ qubits). Based on this idea, an algorithm (Algorithm 1) is developed to compute fault effect $F(\psi_e, \mathcal{E}_f(\psi_t))$. For calculating fidelity with input test states $|\psi_t\rangle$ that have unknown expected output state $|\psi_e\rangle$, since $|\psi_e\rangle = U|\psi_t\rangle$, we can append the tensor network for calculating $U|\psi_t\rangle$ at the end of the tensor network of the faulty circuit. Moreover, we observe that those gates after the last fault can be canceled out, reducing the calculation cost of contracting the tensor network, as shown in Fig. 2.

V. EXPERIMENTS ON SUPERCONDUCTING QUANTUM CIRCUITS

In this section, we demonstrate the utility and effectiveness of our fault simulation algorithm by computing the fault effects of superconducting quantum circuits with realistic fault models introduced before. All types of these circuits have been implemented on quantum superconducting devices of Google.

Runtime Environment: All our experiments are carried out on a server with Intel Xeon Platinum 8153 @ 2.00GHz $\times 256$ Processors, 2048 GB Memory. The machine runs Centos 7.7.1908. We use the Google TensorNetwork Python package [18] for the tensor network computation. The time-out (TO) limit was set to 3600 seconds. The memory-out (MO) limit was set to 2048 GB.

Experimental Cases: We test our fault simulation algorithm by computing the fault effects of three types of practical superconducting quantum circuits which have already been implemented on Google's *Sycamore* quantum superconducting processor: (i) Quantum Approximate Optimization Algorithm (QAOA), (ii) Hartree-Fock Variational Quantum Eigensolver (VQE), and (iii) *inst* circuits used to show the quantum supremacy of *Sycamore* [20], [28], [29]. The test states in all experiments are chosen to be $|0\rangle \otimes \dots \otimes |0\rangle$. To get fidelity results we append the tensor network representing $U|0\rangle \otimes \dots \otimes |0\rangle$, as explained in Section IV. We generate the faulty circuits by putting the unitary fault after each CZ gate or randomly inserting m decoherence noises in the circuits. Thus, the number of unitary faults is that of CZ gates in the circuits, and the number m of super-operator fault is in the range $0 \leq m \leq 16$.

Baselines: We compare the efficiency of our simulator with the simulators of DDSIM [15], Qiskit, and TDD (Tensor Decision Diagram) [30], [31]. The DDSIM is a state-of-the-art DD-based simulator for noiseless circuit simulation, we use it to benchmark

the performance of our simulator in noise-free cases. The algorithm in Qiskit is widely used in quantum simulation and based on matrix-vector techniques, and that of TDD is based on tensor network techniques. All three simulation algorithms are executed on the same runtime environment mentioned above.

Optimization Techniques: One standard method for contracting tensor networks is through a sequential pairwise contraction, i.e., two tensors from the tensor network are selected and merged as one tensor. The tensor network contraction is finished by repeatedly applying the pairwise contraction. A cleverly chosen pairwise contraction order can often reduce tensor network contraction’s runtime by several orders of magnitude. Over the years, many heuristics have been proposed to find efficient orders. Here, we call a greedy method (embedded in Google TensorNetwork) to speed up the tensor network contraction in our algorithm. Other heuristics may further optimize the performance of our algorithm.

Experimental Results and Analysis: The utility and effectiveness of our simulation algorithm are confirmed by the following four numerical experiments (1 – 4) in terms of runtime, fault numbers, fidelity, and the physical parameters (introduced in Section II) appearing in realistic faulty superconducting quantum circuits. For all cases, except for (3), we fix the parameters: the fault rotation angle θ of controlled- $R_z(\theta)$ is chosen to be 0.1, the decoherent time is set to $T_1 = 100\mu\text{s}$ and $T_2 = 20\mu\text{s}$.

The concrete benchmark circuits consist of A -qubit QAOA circuit (qaoa_ A), $B \times C$ -qubit *inst* circuit with depth D (inst_ $B \times C \times D$) and E -qubit Hartree-Fock VQE circuit (hf_ E), where A, B, C, D, E are all positive numbers.

(1) *Super-operator Fault Number and Runtime*: We illustrate the performance of our algorithm with different *super-operator fault numbers* (i.e., the number of super-operator faults in quantum circuits) in Fig. 3. The result shows that our algorithm works very well when the super-operator fault number is small (≤ 6), while, with the super-operator fault number increasing, the runtime grows significantly. The main reason is that more super-operator faults may increase the maximum rank of nodes in the contraction of the tensor network.

(2) *Fault Number and Fidelity*: The relation between fidelity and different super-operator fault numbers is shown in Fig 4. The fault number ranges from 2 to 16. Not surprisingly, the fidelity drops with the fault number increasing.

(3) *Fault Parameters and Fidelity*: We show the fidelity with different parameters in the fault model, including rotation angle θ , T_1 , and T_2 , in Figs. 5 and 6. As a result, larger faulty rotation angles and shorter decoherence time (T_1 and T_2) will lead to a more significant fault effect on superconducting quantum circuits. From Fig. 5, we can say that a larger rotation angle leads to a high loss of fidelity, which is a challenge for hardware technology in the current NISQ era.

(4) *Performance Comparison*: First we compare the performance of our algorithm with the state-of-the-art QMDD-based simulator DDSIM in Table II by running a noiseless simulation task. The result shows that our method outperforms DDSIM in almost all test cases, indicating that our algorithm performs well on the noiseless simulation task of these superconducting quantum circuits. Then, we mainly compare the performance of TDD and our algorithm on the three benchmark circuits in Table III, IV, V. Qiskit can only simulate the Hartree-Fock VQE circuit since the qubit number is small. Although DDSIM can perform faulty circuit simulation [17], the task is slightly different from ours, and the performance is most concerned with stochastic simulation, so it is not compared with our simulator for noisy quantum circuits. The $|\psi_e\rangle$ in this task is chosen

to be $|0\rangle \otimes \dots \otimes |0\rangle$ and the runtime of our algorithm will be the same for any other product states. From our result, our method has less runtime in all three benchmarks than the TDD method with the super-operator fault number set to be 2. The performance of our method is better, especially in *inst* circuits with large depths. The high efficiency of our method results from the fact that our tensor network method utilizes the locality of quantum circuits and several state-of-the-art contracting methods embedded in the Google TensorNetwork package. Since the simulator in Qiskit does not consider the locality, it can only handle circuits with few qubits. Although the TDD method benefits from the locality, the representation is unsuitable for representing a state with arbitrary amplitude on all computational basis (e.g., *inst* circuits). Moreover, the partition strategy used in TDD is straightforward compared to the strategies embedded in the Google TensorNetwork package, which may find more efficient contraction orders.

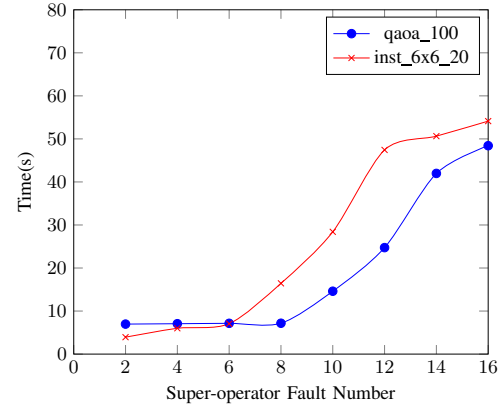


Fig. 3: Super-operator Fault Number and Runtime.

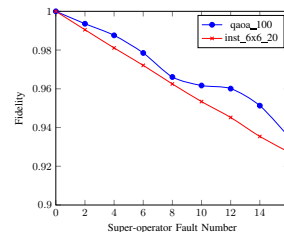


Fig. 4: Super-operator Fault Number and Fidelity

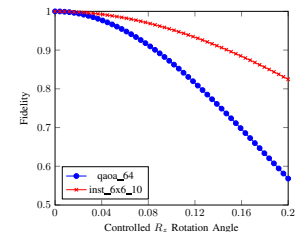


Fig. 5: Unitary Fault Angle and Fidelity

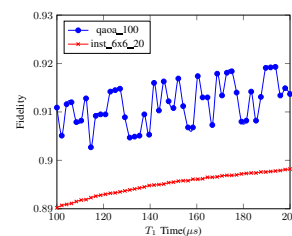


Fig. 6: Decoherence Time and Fidelity

VI. CONCLUSION

This paper presents a fast fault simulation algorithm for quantum superconducting circuits. In particular, we employ tensor network

TABLE II: COMPARISON WITH DDSIM

Circuit	Qubits	Gates	Depth	Time(s)	
				Our	DDSIM
hf_10	10	461	142	0.38	0.20
hf_12	12	690	194	0.88	0.67
qaoa_20	20	188	33	0.09	129.51
qaoa_25	20	241	33	0.12	TO
inst_4x4_60	16	579	61	7.18	26.70
inst_4x4_70	16	669	71	13.48	31.18
inst_4x4_80	16	764	81	18.89	36.69
inst_4x5_10	20	145	11	0.19	242.05
inst_4x5_20	20	261	21	0.27	1839.90
inst_4x5_30	20	378	31	26.98	TO
inst_6x6_10	36	264	11	0.39	TO
inst_6x6_20	36	483	21	3.75	TO
inst_7x7_10	49	364	11	0.43	TO

TABLE III: HARTREE-FOCK RESULT

Circuit	Qubits	Gates	Depth	Time(s)		
				Our	TDD	Qiskit
hf_6	6	155	72	0.095	1.2	0.17
hf_8	8	308	124	0.33	3.65	0.24
hf_10	10	461	142	0.37	7.59	26.91
hf_12	12	690	194	0.99	18.81	206.37

contraction to calculate the fault effect. The utility and effectiveness of our algorithm are demonstrated by experimenting on a series of realistic faulty superconducting circuits. The experimental results indicate that the proposed algorithm (implemented with Google TensorNetwork) significantly improves the efficiency and scalability of the state-of-the-art fault simulation algorithms based on the density matrix or DD-based method, especially for superconducting quantum circuits in the current NISQ era. Therefore, our algorithm is expected to be used as an integrated feature in the currently developed ATPG programs (e.g., [22]–[24]) for verifying and detecting design errors, manufacturing defects, and quantum noise effects of large-size quantum (superconducting) circuits.

REFERENCES

- [1] F. Arute *et al.*, “Quantum supremacy using a programmable superconducting processor,” *Nature*, vol. 574, no. 7779, pp. 505–510, 2019.
- [2] M. Gong *et al.*, “Quantum walks on a programmable two-dimensional 62-qubit superconducting processor,” *Science*, vol. 372, no. 6545, pp. 948–952, 2021.
- [3] J. Preskill, “Quantum computing in the NISQ era and beyond,” *Quantum*, vol. 2, p. 79, 2018.
- [4] M. Abramovici, M. A. Breuer, A. D. Friedman, *et al.*, *Digital systems testing and testable design*. Computer science press New York, 1990, vol. 2.
- [5] L.-T. Wang, C.-W. Wu, and X. Wen, *VLSI test principles and architectures: design for testability*. Elsevier, 2006.
- [6] X.-D. Cai *et al.*, “Experimental quantum computing to solve systems of linear equations,” *Physical Review Letters*, vol. 110, no. 23, p. 230501, 2013.
- [7] A. W. Harrow, A. Hassidim, and S. Lloyd, “Quantum algorithm for linear systems of equations,” *Physical review letters*, vol. 103, no. 15, p. 150502, 2009.
- [8] T. Häner and D. S. Steiger, “5 petabyte simulation of a 45-qubit quantum circuit,” in *Proceedings of the International Conference for High Performance Computing, Networking, Storage and Analysis*, 2017, pp. 1–10.
- [9] C. Huang *et al.*, “Classical simulation of quantum supremacy circuits,” *arXiv preprint arXiv:2005.06787*, 2020.
- [10] R. Li, B. Wu, M. Ying, X. Sun, and G. Yang, “Quantum supremacy circuit simulation on sunway taihulight,” *IEEE Transactions on Parallel and Distributed Systems*, vol. 31, no. 4, pp. 805–816, 2019.
- [11] E. Pednault *et al.*, “Breaking the 49-qubit barrier in the simulation of quantum circuits,” *arXiv preprint arXiv:1710.05867*, vol. 15, 2017.
- [12] B. Villalonga *et al.*, “A flexible high-performance simulator for verifying and benchmarking quantum circuits implemented on real hardware,” *npj Quantum Information*, vol. 5, no. 1, pp. 1–16, 2019.
- [13] F. Pan and P. Zhang, “Simulation of quantum circuits using the big-batch tensor network method,” *Phys. Rev. Lett.*, vol. 128, p. 030501, 3 Jan. 2022. doi: 10.1103/PhysRevLett.128.030501.
- [14] Y.-H. Tsai, J.-H. R. Jiang, and C.-S. Jhang, “Bit-slicing the hilbert space: Scaling up accurate quantum circuit simulation,” in *2021 58th ACM/IEEE Design Automation Conference (DAC)*, San Francisco, CA, USA: IEEE Press, 2021, pp. 439–444. doi: 10.1109/DAC18074.2021.9586191.
- [15] A. Zulehner and R. Wille, “Advanced simulation of quantum computations,” *IEEE Transactions on Computer-Aided Design of Integrated Circuits and Systems*, vol. 38, no. 5, pp. 848–859, 2018.
- [16] S. Hillmich, R. Kueng, I. L. Markov, and R. Wille, “As accurate as needed, as efficient as possible: Approximations in dd-based quantum circuit simulation,” in *2021 Design, Automation & Test in Europe Conference & Exhibition (DATE)*, IEEE, 2021, pp. 188–193.
- [17] T. Grurl, J. Fuß, and R. Wille, “Noise-aware quantum circuit simulation with decision diagrams,” *IEEE Transactions on Computer-Aided Design of Integrated Circuits and Systems*, pp. 1–1, 2022. doi: 10.1109/TCAD.2022.3182628.
- [18] C. Roberts *et al.*, *TensorNetwork: A library for physics and machine learning*, 2019.
- [19] “Fault models in superconducting quantum circuits,” unpublished.
- [20] M. Harrigan *et al.*, “Quantum approximate optimization of non-planar graph problems on a planar superconducting processor,” *Nature Physics*, 2021.
- [21] M. A. Nielsen and I. L. Chuang, *Quantum computation and quantum information*. Cambridge university press, 2010.
- [22] X. Fang-ying, C. Han-wu, L. Wen-jie, and L. Zhi-giang, “Fault detection for single and multiple missing-gate faults in reversible circuits,” in *2008 IEEE Congress on Evolutionary Computation (IEEE World Congress on Computational Intelligence)*, IEEE, 2008, pp. 131–135.

TABLE IV: QAOA RESULT

Circuit	Qubits	Gates	Depth	Time(s)	
				Our	TDD
qaoa_64	64	1696	42	3.512039	58.33
qaoa_72	72	1922	42	4.412076	77.98
qaoa_80	80	2148	42	5.342694	95.34
qaoa_100	100	2720	42	11.64412	149.01
qaoa_121	121	3322	42	9.770204	225.76
qaoa_169	169	4706	42	18.46261	463.89
qaoa_196	196	5488	42	336.4724	617.16
qaoa_225	225	6330	42	925.8719	MO

TABLE V: *inst* RESULT

Circuit	Qubits	Gates	Depth	Time(s)	
				Our	TDD
inst_4x4_10	16	115	11	0.07	0.88
inst_4x4_20	16	209	21	0.20	4.17
inst_4x4_30	16	299	31	5.76	TO
inst_4x4_40	16	394	41	4.34	TO
inst_4x4_50	16	485	51	4.80	TO
inst_4x4_60	16	579	61	9.93	TO
inst_4x4_70	16	669	71	21.72	TO
inst_4x4_80	16	764	81	11.26	TO
inst_4x5_10	20	145	11	0.10	1.52
inst_4x5_20	20	261	21	0.30	TO
inst_4x5_30	20	378	31	30.98	TO
inst_4x5_40	20	494	41	62.29	TO
inst_4x5_50	20	610	51	123.83	TO
inst_4x5_60	20	726	61	1587.82	TO
inst_4x5_70	20	843	71	2027.34	TO
inst_4x5_80	20	959	81	TO(4132.89)	TO
inst_6x6_10	36	264	11	0.22	0.77
inst_6x6_20	36	483	21	4.85	21.41
inst_7x7_10	49	364	11	0.45	1.66

- [23] A. Paler, I. Polian, and J. P. Hayes, "Detection and diagnosis of faulty quantum circuits," in *17th Asia and South Pacific Design Automation Conference*, IEEE, 2012, pp. 181–186.
- [24] D. Bera, "Detection and diagnosis of single faults in quantum circuits," *IEEE Transactions on Computer-Aided Design of Integrated Circuits and Systems*, vol. 37, no. 3, pp. 587–600, 2017.
- [25] J. Biamonte and V. Bergholm, "Tensor networks in a nutshell," *arXiv preprint arXiv:1708.00006*, 2017.
- [26] I. L. Markov and Y. Shi, "Simulating quantum computation by contracting tensor networks," *SIAM Journal on Computing*, vol. 38, no. 3, pp. 963–981, 2008.
- [27] M. Ying, *Foundations of Quantum Programming*. Morgan Kaufmann, 2016.
- [28] Google AI Quantum and Collaborators *et al.*, "Hartree-fock on a superconducting qubit quantum computer," *Science*, vol. 369, no. 6507, pp. 1084–1089, 2020. doi: 10.1126/science.abb9811.
- [29] S. Boixo *et al.*, "Characterizing quantum supremacy in near-term devices," *Nature Physics*, vol. 14, pp. 595–600, 2018.
- [30] X. Hong, X. Zhou, S. Li, Y. Feng, and M. Ying, "A tensor network based decision diagram for representation of quantum circuits," *ACM Trans. Des. Autom. Electron. Syst.*, vol. 27, no. 6, Jun. 2022, ISSN: 1084-4309. doi: 10.1145/3514355.
- [31] X. Hong, M. Ying, Y. Feng, X. Zhou, and S. Li, "Approximate equivalence checking of noisy quantum circuits," in *2021 58th ACM/IEEE Design Automation Conference (DAC)*, 2021, pp. 637–642. doi: 10.1109/DAC18074.2021.9586214.